Macromolecules

Article

Cite This: Macromolecules 2018, 51, 6312−6317

pubs.acs.org/Macromolecules

Blob Size Controls Diffusion of Free Polymer in a Chemically Identical Brush in Semidilute Solution

Zhenyu J. Zhang,[†,‡] Steve Edmondson,[§] Matthew Mears,[†] Jeppe Madsen,[∥] Steven P. Armes,[∥] Graham J. Leggett,[∥] and Mark Geoghegan*[,†]

[†]Department of Physics and Astronomy, University of Sheffield, Sheffield S3 7RH, U.K.

[‡]School of Chemical Engineering, University of Birmingham, Birmingham B15 2TT, U.K.

[§]School of Materials, University of Manchester, Oxford Road, Manchester M13 9PL, U.K.

[∥]Department of Chemistry, University of Sheffield, Sheffield S3 7HF, U.K.

Supporting Information

ABSTRACT: The diffusion of rhodamine-labeled poly(ethylene glycol) (r-PEG) within surface-grafted poly(ethylene glycol) (s-PEG) layers in aqueous solution at 18 °C was measured by fluorescence correlation spectroscopy. The diffusion coefficient of r-PEG within s-PEG was controlled by the grafting density, σ, and scaled as $\sigma^{-1.42\pm0.09}$. It is proposed that a characteristic blob size associated with the grafted (brush) layer defines the region through which the r-PEG diffusion occurs. The diffusion coefficients for r-PEG in semidilute solution were found to be similar to those in the brushes.

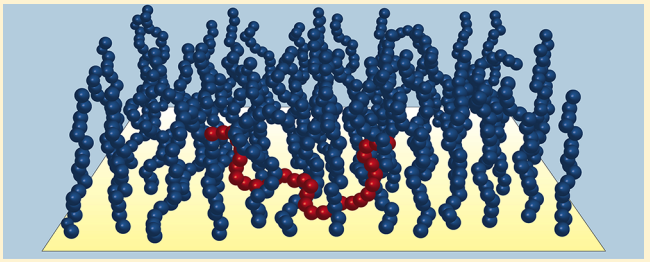

INTRODUCTION

The diffusion of polymer chains in confined environments is an enduring subject in polymer science.[1−10] A deceptively simple problem concerns the diffusion of free chains within chemically identical brushes (surface-grafted chains). Here, confinement is determined by the height of the brush, which may be comparable to that of the dimensions of the diffusing coils. The diffusion of polymer chains trapped within brushes may therefore have different concentration and chain length dependences compared to free chains in solution. Nevertheless, little experimental attention has been given to this problem, partly due to the apparent difficulty in swelling brushes with linear chains.[5,10,11]

The simplest description of polymer brushes in semidilute solutions is that of Alexander and de Gennes[12,13] whereby each brush chain is subdivided into a series of "blobs", the size of which is equal to the distance between grafting points, d. On length scales below that of the blob size, the polymer adopts a self-avoiding walk conformation, but on larger length scales the chain is extended. It is therefore useful to test whether or not the diffusion of free polymers within brushes is governed by the size of these blobs. To achieve this, the size of the diffusing chain must be no larger than the grafted polymers; otherwise, additional confinement effects may arise. Other, more sophisticated, models have since been developed, largely based on the self-consistent mean-field models of Milner, Witten, and Cates,[14,15] which predict a parabolic brush concentration profile.

The penetration of brushes by linear polymers is impeded by the entropic penalty of swelling the brush to accommodate the free chains. This entropic effect is responsible for numerous applications of brushes in the context of colloidal stabilization and surface modification.[16−19] In particular, many hydrophilic polymers exhibit excellent biocompatibility and lubricity, while also preventing protein adsorption when grafted onto planar or colloidal substrates.[18,19] The prototypical coating for biocompatible surfaces is poly(ethylene glycol) (PEG).[20,21] Here, the diffusion of free rhodamine-labeled PEG (r-PEG) chains within a surface-grafted PEG layer (s-PEG) of the same molar mass was measured using fluorescence correlation spectroscopy (FCS) as a function of grafting density. It is shown that the r-PEG diffusion coefficient, D, is related to the grafting density of the s-PEG layer by $D \propto \sigma^{-1.42}$.

FCS allows quantitative measurement of the diffusion of single molecules and requires very dilute labels. Originally developed for use with biological systems, FCS has been used to study synthetic polymers for many years.[22] There has also been a number of FCS studies focused on the diffusion of polymers at surfaces and interfaces.[2,5,6,9]

EXPERIMENTAL SECTION

Brush layers were created by the adsorption of thiol-terminated PEG onto a gold-coated substrate, which has previously been shown to

Received: June 6, 2018
Revised: July 26, 2018
Published: August 10, 2018

DOI: 10.1021/acs.macromol.8b01193
Macromolecules 2018, 51, 6312−6317

create reliable and uniform surfaces.[23−27] Uniform monohydroxy-terminated PEG (PEG-OH, 20 kDa) and uniform monothiol-terminated PEG (PEG-SH, 20 kDa) were purchased from Sigma and Jenkem, respectively.

Rhodamine is a relatively hydrophilic dye,[28,29] at least at neutral pH, which makes it ideal for diffusion measurements such as these. Hydrolyzed rhodamine 6G[28] was reacted with thionyl chloride to form rhodamine 6G acid chloride, 10.0 mg of which was added to 0.5 g of PEG-OH in 5.0 mL of dichloromethane, after which triethylamine (1 mL, 0.73 g) was added. The reaction mixture was stirred overnight at 20 °C. The solvent was evaporated under reduced pressure, and the solid residue was dissolved in water. The red solution was dialyzed against methanol and then water until a colorless dialysate persisted.

Silicon wafers (approximately 1 cm × 5 cm), silicon nitride triangular atomic force microscope (AFM) cantilevers, and all glassware were cleaned in piranha solution. (*Care is required: piranha solution can spontaneously detonate upon contact with organic material.*) The silicon wafers and glassware were rinsed thoroughly with deionized (DI) water six times and sonicated for 10 min before placing in an oven at 80 °C overnight. Cantilevers were rinsed using DI water, dried under nitrogen flow, and stored in an oven at 80 °C. To coat the substrates or cantilevers with a thin film of gold, 5 nm of chromium was deposited on silicon substrates (1 nm on cantilevers) as an adhesive layer at ∼0.02 nm s^{-1}. These were allowed to cool prior to an ∼0.03 nm s^{-1} deposition of 12 or 60 nm thick gold coatings for cantilevers and substrates, respectively.

To vary the grafting density of PEG,[25] SH- and OH-terminated PEG were dissolved together in ultrapure water (HPLC grade, purchased from Sigma-Aldrich). A series of six solutions were prepared by varying the concentration of PEG-OH from 0 to 50% (w/w) in steps of 10%, while the concentration of PEG-SH was maintained at 0.01 g/mL. Gold-coated silicon strips were immersed in these PEG solutions for 24 h. PEG-SH irreversibly adsorbs to the gold, and the PEG-OH screens excluded volume, allowing greater grafting densities than would otherwise be possible. Subsequently, samples were removed from solution, rinsed with water, and dried with nitrogen, before being immersed in chloroform and sonicated for 10 min to remove any unbound PEG. The samples were then rinsed with ultrapure water, dried under nitrogen, and stored in degassed ethanol. The strips were then cut into 1 cm × 1 cm pieces prior to any measurements, rinsed with copious ethanol, and dried with nitrogen. The brushes were observed to be stable on experimental time scales given that there were no observed changes in diffusion during the experiments and that the force spectroscopy measurements of thickness were reproducible. Recent quartz-crystal microbalance data have been used to demonstrate the stability of thiol-terminated PEG layers on gold.[27] Gold-coated AFM cantilevers were also incubated in PEG-SH solution, providing a low grafting density s-PEG layer on the cantilever for force spectroscopy experiments.

A J.A. Woollam multiwavelength ellipsometer was used to measure the thicknesses (both dry and in water) of the PEG brush layers on the gold-coated silicon wafer. A gold-coated wafer without a PEG coating was used to fit substrate optical properties. The dry thickness of each PEG brush layer was fitted using a Cauchy layer for the PEG brush, with a refractive index given by $1.45 + 0.01/\lambda^2$, where the wavelength, λ, is in micrometers. Ellipsometry measurements were performed over three positions on the same sample, and the mean thickness was converted to grafting density, σ, using 1.13 g cm^{-3} for the dry PEG density. The data from water-swollen PEG brushes in a liquid cell were fitted using a single-layer linear effective medium approximation model (comprising water and PEG, with the stated Cauchy parameters), after fitting the cell window offsets using a dry sample. Here $\sigma = v^{2/3}/d^2$ is the dimensionless areal density of grafting points, where v is the monomer volume.

Complementary (aqueous) thickness measurements of s-PEG layers were obtained using force spectroscopy. These measurements were performed using a Multimode atomic force microscope equipped with a Nanoscope IV controller using Nanoscope 5.31 software (Veeco), operating in contact mode using gold-coated AFM cantilevers and PEG brushes on gold-coated silicon substrates. The spring constants of the cantilevers were calibrated from their thermal spectra.[30]

The ellipsometric thicknesses of (dry) s-PEG brush layers are presented in Figure 1. The samples were prepared with the immersion of gold-coated silicon wafers in PEG mixture solutions of different weight fractions of PEG-OH, which ranged from 0 to 50%. As expected, the thickness of the immobilized PEG brush layer increased when using larger PEG-OH fractions in the binary PEG solution, in agreement with previous work using the same methodology.[25]

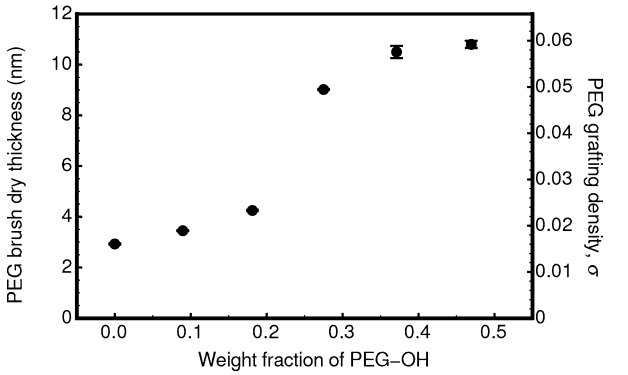

Figure 1. Dry thickness of s-PEG measured by ellipsometry and the corresponding grafting density as a function of weight fraction of PEG-OH used during preparation of the brush. The transition at which the excluded volume interaction is suppressed occurs between 20% and 30% PEG-OH.

Measuring the thickness of a brush in solution is not trivial, although it can be obtained relatively reliably with neutron reflectometry.[31] Here, ellipsometry and force spectroscopy were used to obtain the mean brush thickness. Lack of contrast between the brush and water meant that ellipsometry could only be used for the four most densely grafted brushes. The mean thickness could however be determined for all brushes using force spectroscopy, following an earlier methodology.[32−34] In this case the brush thickness was taken to be the onset of the repulsive force in the approach curve, i.e., the point at which the repulsive force is midway between one and two standard deviations above the noise in the force curve (Figure 2a). These AFM experiments were readily reproducible over different positions, which means that the brush coverage of the surface was uniform.

Dense polymer brushes must swell to allow other polymers to enter and the associated entropic cost limits the amount of swelling that is possible. In the experiments reported in this work, the grafted layers are brushes, but not strongly stretched ones. The average distance between grafting points varies from 1.6 to 3.2 nm in the experiments described herein, which compares with the hydrodynamic radius of the PEG in dilute solution of 2.4 nm. (The hydrodynamic radius of r-PEG was calculated using the Stokes−Einstein equation and D = 96.7 μm^2 s^{-1}.) It is therefore not unrealistic for individual polymers to enter the brush. To understand the interaction of PEG in solution with the brush layer, force spectroscopy experiments were performed using a PEG-coated tip (σ = 0.016, assuming a similar brush growth to those on the gold-coated silicon surfaces). The PEG-coated tip readily penetrated a lightly grafted brush layer resulting in a 2 nm pull-off force (Figure 2b). No such attractive force was observed when separating a gold-coated tip from a PEG layer, which confirms that the adhesion force measured is due to the interaction between the two PEG layers. However, when the PEG-coated tip was brought toward a more densely grafted layer (σ = 0.059), it was unable to penetrate, at least with an applied force of 15 nN, and instead a long-range repulsion was observed. It can be concluded from these data that there is an energy barrier to PEG entering the brush layer. This energy barrier does not preclude PEG entering the brush, which would be expected to be a rare occurrence, but certainly it does mean that the

DOI: 10.1021/acs.macromol.8b01193
Macromolecules 2018, 51, 6312−6317

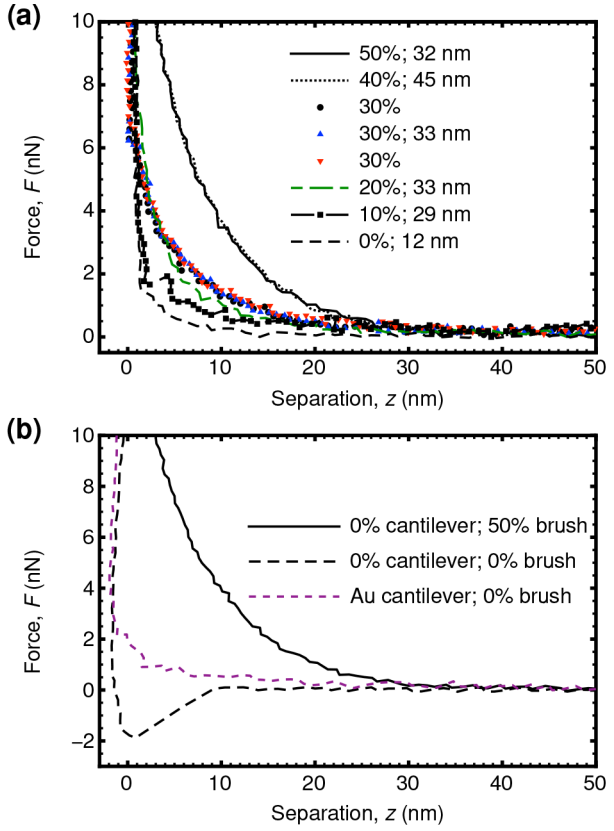

Figure 2. (a) Force spectroscopy approach curves for a gold-coated AFM tip compressing the upper surface of a PEG brush for various grafting densities. The repulsive force increases at larger distances for denser brushes. The legend indicates the quantity of PEG-OH used to screen excluded volume in the preparation of the brush and the brush layer thickness obtained from the onset of repulsion, where 0%, for example, indicates that no PEG-OH was used to screen excluded volume in the preparation of the brush layer. Three curves are shown for the 30% brush (i.e., 30% of the PEG used in preparing the brush was PEG-OH) to illustrate the reproducibility of the data. (b) Force spectroscopy retraction curves for a gold-coated AFM tip leaving a PEG-brush with the smallest grafting density and two PEG-coated AFM tips (smallest grafting density) from two surface-grafted PEG layers with different grafting densities (σ = 0.016 and 0.059). The experiments in both figures were performed until F = 15 nN was achieved, and the retraction was performed immediately on achieving this force.

diffusion of PEG atop the brush is unlikely. Recent experiments on a PEG-modified glass surface have shown that PEG does not adsorb to these surfaces.[35] The dominant diffusive processes of the r-PEG are therefore in bulk solution or within the s-PEG layer.

The FCS experiment is performed at very low concentrations of r-PEG, with approximately one dye label within the confocal volume at any one time. A dilute aqueous r-PEG solution (10 nM) was prepared immediately before each measurement. For measurements of r-PEG diffusion in (bulk) semidilute solution, r-PEG was diluted to 10 nM in PEG-OH solutions. FCS measurements were made using a ConfoCor 2 FCS module fitted to an LSM510 inverted confocal microscope (Zeiss) and a water-immersed objective (C-Apochromat 40×/1.2 W Korr).

FCS measurements were made using a ConfoCor 2 FCS module fitted to an LSM510 inverted confocal microscope (Zeiss). All measurements were performed at 18 °C. The rhodamine 6G label of r-PEG was excited using the 514 nm line of an argon laser. Extraneous fluorescence emission was rejected using a 530−600 nm band-pass filter, and the rest was recorded with an avalanche photodiode. Photobleaching was inhibited by attenuation of the laser using a neutral density filter. Fluctuations in the fluorescence signal from dye-labeled molecules were quantified by autocorrelation of the fluorescence intensity signal. The width of the confocal volume was calibrated by conducting diffusion measurements using 10 nM rhodamine 6G whose diffusion rate is 426 $\mu m^2\ s^{-1}$ at 22.5 ± 0.5 °C.[36]

For FCS surface diffusion measurements, PEG functionalized gold substrates were placed on a coverslip, facing downward, with a spacer (Grace Bio-Laboratories SecureSeal, Sigma-Aldrich, Dorset, UK) to keep them apart and accommodate sufficient amount of liquid. The PEG brush samples were allowed to equilibrate for 30 min before measuring. The z-scanning was performed in steps of 30 nm from the bulk solution toward the surface using the automated stage positioning of the ConfoCor 2 system until the signal-to-noise ratio was maximized. This ensures that the autocorrelation curves of the best quality can be achieved. The raw autocorrelation curves acquired were fitted to

$$G(\tau) = 1 + \frac{G_{\text{triplet}}(\tau)}{n}\left(\frac{1-f}{\left(1+\frac{\tau}{\tau_{3D}}\right)\sqrt{1+\frac{\tau}{\tau_{3D}S^2}}} + \frac{f}{1+\frac{\tau}{\tau_{2D}}}\right) \quad (1)$$

using a Monte Carlo algorithm to determine the starting parameters and a Levenberg−Marquardt routine to determine best-fit parameters. Here G_{triplet} represents the contribution to the triplet fluorescence decay and is significant at short times only; f is the fraction of dye molecules in the surface layer (i.e., the brush); τ is the decay time; τ_{3D} and τ_{2D} are the time constants for bulk and confined diffusion; n is the number of dye molecules within the confocal volume; and S^2 is a geometrical parameter associated with the shape of the confocal volume. The triplet decay occurs on the shortest time scales, followed by the bulk diffusion and the surface diffusion, which is important at the longest times. As a consequence, $G(\tau)$ can discriminate between two- and three-dimensional diffusion,[37] which enabled determination of the diffusion coefficient of r-PEG in s-PEG. This diffusion is here deemed surface diffusion, but it is not a constrained two-dimensional diffusion but rather a three-dimensional diffusion within a narrow layer. Because the brush layer is thin compared to the confocal volume, it is treated in eq 1 as two-dimensional diffusion.

Before the surface diffusion was measured, the PEG brush layer was allowed to absorb r-PEG for 30 min. Given the geometry of the confocal volume, it is expected that bulk r-PEG diffusion contributes to the total fluorescence signal during measurements. However, bulk and surface diffusion are sufficiently dissimilar that these two components of the autocorrelation curve could be resolved and the two diffusion coefficients easily extracted. Measurements in solution also provide a diffusion coefficient for bulk diffusion, allowing this parameter to be constrained. The diffusion coefficient of the 20 kDa r-PEG chains in dilute (10 nM) solution was measured to be 97 ± 5 $\mu m^2\ s^{-1}$, which is consistent with earlier work.[2] In fitting the surface diffusion, the bulk diffusion coefficient was held fixed to within 10%. The number of molecules confined within the brush layer decreased by a factor of ∼6 as the grafting density increased.

RESULTS AND DISCUSSION

FCS data and fits are shown in Figure 3 along with the diffusion coefficients obtained from fitting the autocorrelation data. The diffusion of PEG in the brushes is presented as a function of grafting density in Figure 3b. This double-logarithmic plot shows that a power law behavior can reasonably describe the diffusion, and the fit shows that the diffusion coefficient scales with grafting density as $D \propto \sigma^{-1.42}$. The fraction of the signal due to the brush-absorbed polymers is typically between 5% and 10%, but because the bulk diffusion is considerably faster than the surface diffusion, these are easily separable in the fitting. In Figure 3c the areal density of polymers absorbed by the brush is presented, showing that

DOI: 10.1021/acs.macromol.8b01193
Macromolecules 2018, 51, 6312−6317

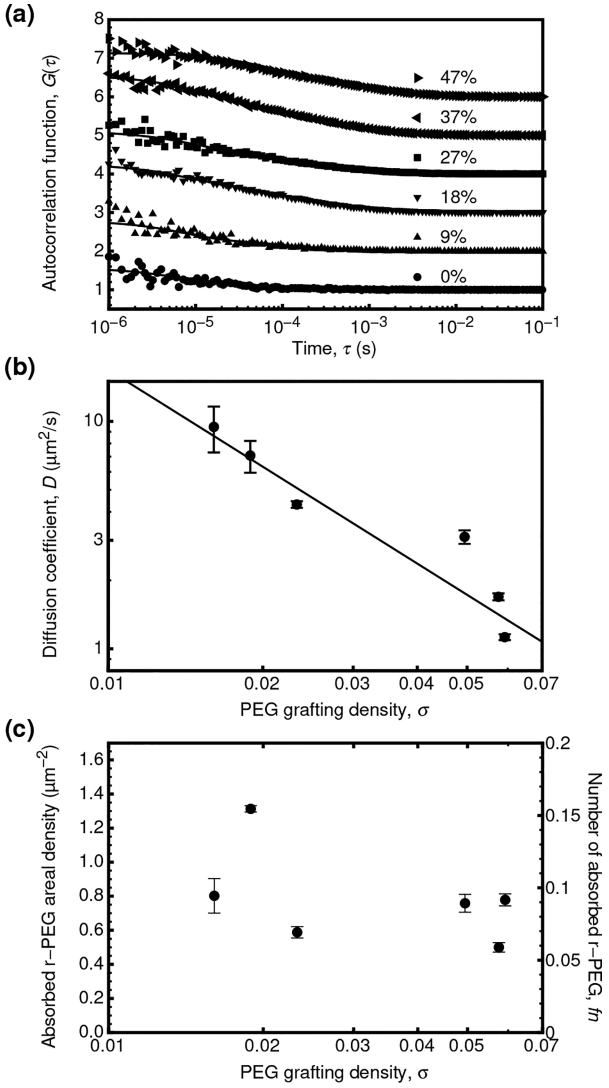

Figure 3. (a) FCS data and fits for r-PEG diffusing in an s-PEG layer. The legend states the quantity of PEG-OH used to screen excluded volume in the preparation of the brush for each data set. The data are vertically offset for clarity; in each case, $G(\tau) \rightarrow 1$ for large τ. (b) Surface diffusion coefficients obtained from the fits to the FCS data. The solid line is a fit to the data, which yields $D \propto \sigma^{-n_s}$, where $n_s = 1.42 \pm 0.09$. The uncertainty in grafting density (not shown) is taken to be 5%. (c) Areal density of r-PEG absorbed by the brush (number of r-PEG per μm^2), as obtained from the fits to the FCS data. The number of r-PEG molecules absorbed by the brush within the confocal volume is indicated on the right-hand axis. This is the total number of r-PEG chains in the confocal volume, n, multiplied by the fraction of those in the brush, f. The error bars are calculated assuming that n and f are independent parameters.

any grafting density dependence of the absorbed amount is hard to determine. Although PEG-grafted surfaces provide antifouling coatings,[21] they do not work indefinitely. For the same reason, although PEG is repelled from the s-PEG layer (Figure 2b), it will occasionally penetrate it. A small quantity of r-PEG is therefore absorbed by the s-PEG. This quantity represents a greater concentration than the 10 nM solution above it, which is a result of the polymer motion slowing down within the brush, due to the obstacles inhibiting its escape. In fitting the data, it was found that because $f \ll 1 - f$, it could vary significantly in the fitting. The surface diffusion coefficient, however, was a robust fitting parameter whose values were determined within a narrow range.

A detailed balance must exist between r-PEG within the brush and in the solution above it, but FCS cannot here reveal the rate of r-PEG leaving or entering the brush. Any r-PEG that left the brush, even if only temporarily, contributed to bulk diffusion and was assessed as such. An "interphase" contribution[35] was not observed in these experiments. Although FCS is capable of measuring multiple diffusion coefficients, it is not capable of evaluating the nature of the different processes involved in the diffusion and tracking techniques would be more appropriate.[9,38,39] The conclusion that the rate of entering and leaving the brush is small is consistent with other experiments which showed that PEG diffusion could be measured in the vicinity of weakly attractive self-assembled monolayers, but not a PEG-modified surface.[35] The diffusion coefficient of r-PEG on a clean gold surface, i.e., without the adsorbed brush, was measured to be 11.7 ± 1.5 $\mu m^2\ s^{-1}$. This large value reflects a relatively unconstrained diffusion on a hydrophilic surface.

To compare the diffusion data for r-PEG in brushes with those for r-PEG in semidilute solution, measurements of the self-diffusion of r-PEG were performed in the presence of varying amounts of PEG-OH, ranging from the dilute to the semidilute regime. The diffusion coefficient of r-PEG in solution is presented in Figure 4 as a function of the

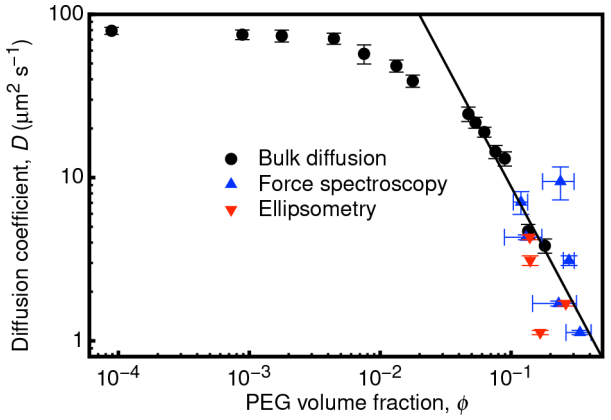

Figure 4. Self-diffusion coefficients (circles), D, for r-PEG in aqueous solutions of PEG of varying PEG concentrations. The solid line is a fit to the data for $\phi > 0.03$, which yields $D \propto \phi^{-n}$, where $n = 1.50 \pm 0.08$. The diffusion coefficients shown in Figure 3b are also included, whereby ϕ was calculated by considering brush thicknesses measured using ellipsometry or force spectroscopy.

concentration of PEG-OH. Diffusion is independent of PEG concentration in dilute solutions, where $\phi < 0.002$. (The point at which chains start to overlap is given by $\phi^* \approx \nu N/(4\pi\nu N^{9/5}/3) \approx 0.002$.) At $\phi > 0.03 \approx \nu N/R_G^3$ (R_G is the polymer radius of gyration), the self-diffusion scales as $\phi^{-1.50}$. These PEG-OH concentrations (up to $\phi = 0.18$, the largest used here) cover a range of semidilute solution similar to those for large molar mass polystyrene in earlier experiments,[40] where a scaling relation of $D \propto \phi^{-1.7\pm0.1}$ was observed. The discrepancy between this exponent and that measured here is due to the high molar mass polystyrene exhibiting dynamics due to reptation.[41] The diffusion coefficients for r-PEG in brushes are included in Figure 4, and these are similar to the bulk measurements in semidilute solution at the same concen-

DOI: 10.1021/acs.macromol.8b01193
Macromolecules 2018, 51, 6312−6317

tration, from which it is concluded that the PEG must be within the brush layer, rather than on top of it.

The concept of blobs is based on the polymers exhibiting a self-avoiding random walk conformation on length scales less than the distance between grafting points and is based on a step-function thickness profile. This rather unsophisticated approach has been replaced by self-consistent methods,[15] which provide volume fraction profiles that have a parabolic form, although it has been argued that the osmotic pressure behaviors of both models are similar.[42] The parabolic profile is incompatible with uniform blobs because the blob size would increase with distance from the substrate commensurate with an increase in dilution. Here, however, the free polymer is the same molar mass as the end-grafted chains and so is an inappropriate probe of any parabolic concentration profile of the brush. It is therefore sufficient to conclude that the results described herein do not preclude a parabolic volume fraction profile, merely that the Alexander–de Gennes model is sufficient to describe the data.

The diffusion of a polymer chain in a medium is countered by a frictional force due to that medium, which is proportional to the density of obstacles. In a high molar mass polymer melt or a concentrated polymer solution, these obstacles are chain entanglements. For surface diffusion this frictional force is proportional to σ; a related brush thickness dependence has been observed for polymer surface diffusion on brushes.[5] Within the brush layer the frictional force should scale as $\sigma^{3/2}$. This is because there is one obstacle to diffusion per blob, whereby the brush grafting density defines the blob size (volume $v\sigma^{-3/2}$).[12,13] The diffusion coefficient is close to being inversely proportional to the blob size $\sigma^{3/2}$, as shown in Figure 3b.

CONCLUSIONS

In summary, free PEG chains can overcome the energy barrier introduced by the PEG brush and diffuse within a PEG brush layer. The diffusion coefficient scales with the brush grafting density as $\sigma^{-1.42\pm0.09}$, which indicates that the blob volume controls the diffusion of free polymers within the brush layer.

ASSOCIATED CONTENT

Supporting Information

The Supporting Information is available free of charge on the ACS Publications website at DOI: 10.1021/acs.macromol.8b01193.

A sample z-scan used for calibrating the FCS surface experiment, autocorrelation data and fit for the diffusion of r-PEG on the gold-coated surface (i.e., no brush), and tabulated figure data (PDF)

AUTHOR INFORMATION

Corresponding Author

*(M.G.) E-mail mark.geoghegan@sheffield.ac.uk; Ph +44 (0) 114 2223544; Fax +44 (0)114 2223555.

ORCID

Zhenyu J. Zhang: 0000-0003-0243-2109
Steven P. Armes: 0000-0002-8289-6351
Graham J. Leggett: 0000-0002-4315-9076
Mark Geoghegan: 0000-0001-9919-7357

Notes

The authors declare no competing financial interest.

ACKNOWLEDGMENTS

We acknowledge financial support from the Engineering and Physical Sciences Research Council (EPSRC) under programme grant EP/I012060/1. M.M. was funded by the EPSRC through a PhD studentship and then a doctoral prize fellowship. S.P.A. acknowledges the ERC for a five-year Advanced Investigator grant (PISA: 320372).

REFERENCES

(1) Manias, E.; Chen, H.; Krishnamoorti, R.; Genzer, J.; Kramer, E. J.; Giannelis, E. P. Intercalation kinetics of long polymers in 2 nm confinements. *Macromolecules* **2000**, *33*, 7955–7966.

(2) Sukhishvili, S. A.; Chen, Y.; Müller, J. D.; Gratton, E.; Schweizer, K. S.; Granick, S. Diffusion of a polymer 'pancake'. *Nature* **2000**, *406*, 146.

(3) Ritchie, K.; Shan, X.-Y.; Kondo, J.; Iwasawa, K.; Fujiwara, T.; Kusumi, A. Detection of non-Brownian diffusion in the cell membrane in single molecule tracking. *Biophys. J.* **2005**, *88*, 2266–2277.

(4) Desai, T. G.; Keblinski, P.; Kumar, S. K.; Granick, S. Molecular-dynamics simulations of the transport properties of a single polymer chain in two dimensions. *J. Chem. Phys.* **2006**, *124*, 084904.

(5) Wang, W.; Zhang, C.; Wang, S.; Zhao, J. Diffusion of single polyelectrolytes on the surface of poly(*N*-isopropylacrylamide) brushes. *Macromolecules* **2007**, *40*, 9564–9569.

(6) Burgos, P.; Zhang, Z.; Golestanian, R.; Leggett, G. J.; Geoghegan, M. Directed single molecule diffusion triggered by surface energy gradients. *ACS Nano* **2009**, *3*, 3235–3243.

(7) Chen, R.; Li, L.; Zhao, J. Single chain diffusion of poly(ethylene oxide) in Its monolayers before and after crystallization. *Langmuir* **2010**, *26*, 5951–5956.

(8) Graham, M. D. Fluid dynamics of dissolved polymer molecules in confined geometries. *Annu. Rev. Fluid Mech.* **2011**, *43*, 273–298.

(9) Mears, M.; Tarmey, D. S.; Geoghegan, M. Single macromolecule diffusion in confined environments. *Macromol. Rapid Commun.* **2011**, *32*, 1411–1418.

(10) Wang, S.; Jing, B.; Zhu, Y. Molecule motion at polymer brush interfaces from single-molecule experimental perspectives. *J. Polym. Sci., Part B: Polym. Phys.* **2014**, *52*, 85–103.

(11) Schuh, C.; Rühe, J. Penetration of polymer brushes by chemical nonidentical free polymers. *Macromolecules* **2011**, *44*, 3502–3510.

(12) Alexander, S. Adsorption of chain molecules with a polar head. A scaling description. *J. Phys. (Paris)* **1977**, *38*, 983–987.

(13) de Gennes, P. G. Conformations of polymers attached to an interface. *Macromolecules* **1980**, *13*, 1069–1075.

(14) Milner, S. T.; Witten, T. A.; Cates, M. E. Theory of the grafted polymer brush. *Macromolecules* **1988**, *21*, 2610–2619.

(15) Milner, S. T.; Witten, T. A.; Cates, M. E. A parabolic density profile for grafted polymers. *Europhys. Lett.* **1988**, *5*, 413–418.

(16) Milner, S. T. Polymer brushes. *Science* **1991**, *251*, 905–914.

(17) Zhao, B.; Brittain, W. J. Polymer brushes: surface-immobilized macromolecules. *Prog. Polym. Sci.* **2000**, *25*, 677–710.

(18) Hucknall, A.; Rangarajan, S.; Chilkoti, A. In pursuit of zero: Polymer brushes that resist the adsorption of proteins. *Adv. Mater.* **2009**, *21*, 2441–2446.

(19) Krishnamoorthy, M.; Hakobyan, S.; Ramstedt, M.; Gautrot, J. E. Surface-initiated polymer brushes in the biomedical field: applications in membrane science, biosensing, cell culture, regenerative medicine and antibacterial coatings. *Chem. Rev.* **2014**, *114*, 10976–1026.

(20) Alcantar, N. A.; Aydil, E. S.; Israelachvili, J. N. Polyethylene glycol-coated biocompatible surfaces. *J. Biomed. Mater. Res.* **2000**, *51*, 343–351.

(21) Banerjee, I.; Pangule, R. C.; Kane, R. S. Antifouling coatings: recent developments in the design of surfaces that prevent fouling by proteins, bacteria, and marine organisms. *Adv. Mater.* **2011**, *23*, 690–718.

DOI: 10.1021/acs.macromol.8b01193
Macromolecules 2018, 51, 6312–6317

(22) Koynov, K.; Butt, H.-J. Fluorescence correlation spectroscopy in colloid and interface science. *Curr. Opin. Colloid Interface Sci.* **2012**, *17*, 377−387.
(23) Tokumitsu, S.; Liebich, A.; Herrwerth, S.; Eck, W.; Himmelhaus, M.; Grunze, M. Grafting of alkanethiol-terminated poly(ethylene glycol) on gold. *Langmuir* **2002**, *18*, 8862−8870.
(24) Unsworth, L. D.; Tun, Z.; Sheardown, H.; Brash, J. L. Chemisorption of thiolated poly(ethylene oxide) to gold: surface chain densities measured by ellipsometry and neutron reflectometry. *J. Colloid Interface Sci.* **2005**, *281*, 112−121.
(25) Taylor, W.; Jones, R. A. L. Producing high-density high-molecular-weight polymer brushes by a "grafting to" method from a concentrated homopolymer solution. *Langmuir* **2010**, *26*, 13954−13958.
(26) Emilsson, G.; Schoch, R. L.; Feuz, L.; Höök, F.; Lim, R. Y. H.; Dahlin, A. B. Strongly stretched protein resistant poly(ethylene glycol) brushes prepared by grafting-to. *ACS Appl. Mater. Interfaces* **2015**, *7*, 7505−7515.
(27) Ortiz, R.; Olsen, S.; Thormann, E. Salt-induced control of the grafting density in poly(ethylene glycol) brush layers by a grafting-to approach. *Langmuir* **2018**, *34*, 4455−4464.
(28) Madsen, J.; Warren, N. J.; Armes, S. P.; Lewis, A. L. Synthesis of rhodamine 6G-based compounds for the ATRP synthesis of fluorescently labeled biocompatible polymers. *Biomacromolecules* **2011**, *12*, 2225−2234.
(29) Mottram, L. F.; Forbes, S.; Ackley, B. D.; Peterson, B. R. Hydrophobic analogues of rhodamine B and rhodamine 101: potent fluorescent probes of mitochondria in living *C. elegans*. *Beilstein J. Org. Chem.* **2012**, *8*, 2156−2165.
(30) Hutter, J. L.; Bechhoefer, J. Calibration of atomic-force microscope tips. *Rev. Sci. Instrum.* **1993**, *64*, 1868−1873.
(31) Currie, E. P. K.; Wagemaker, M.; Cohen Stuart, M. A.; van Well, A. A. Structure of monodisperse and bimodal brushes. *Macromolecules* **1999**, *32*, 9041−9050.
(32) Kelley, T. W.; Schorr, P. A.; Johnson, K. D.; Tirrell, M.; Frisbie, C. D. Direct force measurements at polymer brush surfaces by atomic force microscopy. *Macromolecules* **1998**, *31*, 4297−4300.
(33) Yamamoto, S.; Ejaz, M.; Tsujii, Y.; Fukuda, T. Surface interaction forces of well-defined, high-density polymer brushes studied by atomic force microscopy. 2. Effect of graft density. *Macromolecules* **2000**, *33*, 5608−5612.
(34) McLean, S. C.; Lioe, H.; Meagher, L.; Craig, V. S.; Gee, M. L. Atomic force microscopy study of the interaction between adsorbed poly(ethylene oxide) layers: Effects of surface modification and approach velocity. *Langmuir* **2005**, *21*, 2199−2208.
(35) Weger, L.; Weidmann, M.; Ali, W.; Hildebrandt, M.; Gutmann, J. S.; Hoffmann-Jacobsen, K. Polymer diffusion in the interphase between surface and solution. *Langmuir* **2018**, *34*, 7021−7027.
(36) Petrášek, Z.; Schwille, P. Precise measurement of diffusion coefficients using scanning fluorescence correlation spectroscopy. *Biophys. J.* **2008**, *94*, 1437−1448.
(37) Krichevsky, O.; Bonnet, G. Fluorescence correlation spectroscopy: the technique and its applications. *Rep. Prog. Phys.* **2002**, *65*, 251−297.
(38) Skaug, M. J.; Mabry, J. N.; Schwartz, D. K. Single-molecule tracking of polymer surface diffusion. *J. Am. Chem. Soc.* **2014**, *136*, 1327−1332.
(39) Miller, H.; Zhou, Z.; Shepherd, J.; Wollman, A. J. M.; Leake, M. C. Single-molecule techniques in biophysics: a review of the progress in methods and applications. *Rep. Prog. Phys.* **2018**, *81*, 024601.
(40) Hervet, H.; Léger, L.; Rondelez, F. Self-diffusion in polymer solutions: A test for scaling and reptation. *Phys. Rev. Lett.* **1979**, *42*, 1681−1684.
(41) De Gennes, P. G. Dynamics of entangled polymer solutions. II. Inclusion of hydrodynamic interactions. *Macromolecules* **1976**, *9*, 594−598.
(42) Kenworthy, A. K.; Hristova, K.; Needham, D.; McIntosh, T. J. Range and magnitude of the steric pressure between bilayers containing phospholipids with covalently attached poly(ethylene glycol). *Biophys. J.* **1995**, *68*, 1921−1936.

DOI: 10.1021/acs.macromol.8b01193
Macromolecules 2018, 51, 6312−6317